Computers and Electronics in Agriculture 216 (2024) 108513

Contents lists available at ScienceDirect

Computers and Electronics in Agriculture

journal homepage: www.elsevier.com/locate/compag

Original papers

Maximizing value yield in wood industry through flexible sawing and product grading based on wane and log shape

Kamran Forghani [a,*], Mats Carlsson [b], Pierre Flener [a], Magnus Fredriksson [c], Justin Pearson [a], Di Yuan [a]

[a] Department of Information Technology, Uppsala University, Uppsala, Sweden
[b] Department of Computer Science, RISE Research Institutes of Sweden, Gothenburg, Sweden
[c] Department of Engineering Sciences and Mathematics, Luleå University of Technology, Luleå, Sweden

ARTICLE INFO

Keywords:
Sawing optimization
Wood industry
Maximum set packing
Dynamic programming
Parallel processing

ABSTRACT

The optimization of sawing processes in the wood industry is critical for maximizing efficiency and profitability. The introduction of computerized tomography scanners provides sawmill operators with three-dimensional internal models of logs, which can be used to assess value and yield more accurately. We present a methodology for solving the sawing optimization problem employing a flexible sawing scheme that allows greater flexibility in cutting logs into products while considering product quality classes influenced by wane defects. The methodology has two phases: preprocessing and optimization. In the preprocessing phase, two alternative algorithms are given that generate and evaluate the potential sawing positions of products by considering the 3D surface of the log, product size requirements, and product quality classes. In the optimization phase, a maximum set-packing problem is solved for the preprocessed data using mixed-integer programming (MIP), aiming to obtain a feasible cut pattern that maximizes value yield. This is implemented in a system named FlexSaw, which takes advantage of parallel computation during the preprocessing phase and utilizes a MIP solver during the optimization phase. The proposed sawing methods are evaluated on the Swedish Pine Stem Bank. Additionally, FlexSaw is compared with an existing tool that utilizes cant sawing. Results demonstrate the superiority of flexible sawing. While the practical feasibility of implementing a flexible way of sawing logs is constrained by the limitations of current sawmill machinery, the potential increase in yield promotes the exploration of alternative machinery in the wood industry.

1. Introduction

Sawing optimization is the process of maximizing the yield of wooden products from a log by cutting the log into the optimal size and shape. By optimizing the sawing process, the wood industry can reduce the amount of waste, which helps to conserve natural resources and reduce environmental impact. Additionally, sawing optimization helps to improve the quality of wooden products and expand their utility for a wider range of applications.

The introduction of computerized tomography (CT) scanning technology in the wood industry has made it possible to create detailed 3D models depicting the surface and internal defects of logs (Johansson, 2013). This allows sawmill operators to optimize the sawing process by selecting the best cutting pattern and positioning for each log, based on factors such as size, shape, and defects. Thus, this allows sawmills to increase profitability and achieve more consistent product quality.

Regarding the problem of sawing optimization, various approaches have been proposed in the literature. These approaches can be broadly classified into two categories: applying a sawing simulator system, and using mathematical modeling techniques and optimization algorithms. Sawing simulators can be used to evaluate different sawing schemes and optimize the sawing process based on input parameters such as log diameter, log length, log positioning, saw kerf (thickness of its blade), and cut pattern. Some of the sawing simulators used in the wood industry and academia include SAWSIM, SIMSAW, Autosaw, Optsaw, Saw2003, WoodCIM, and Optitek surveyed in Wery et al. (2018). As for mathematical modeling techniques, different methods have been developed to address the sawing optimization problem. However, the most common ones involve mixed integer programming (MIP), dynamic programming, and heuristics.

In the wood industry, the terms board and lumber are used to refer to different types of wooden products (Hosseini and Peer, 2022). A *board*, also called *timber*, typically refers to a relatively narrow and thin piece of wood that is normally cut to a specific width and

* Corresponding author.
E-mail address: kamran.forghani@it.uu.se (K. Forghani).

https://doi.org/10.1016/j.compag.2023.108513
Received 12 July 2023; Received in revised form 2 December 2023; Accepted 4 December 2023

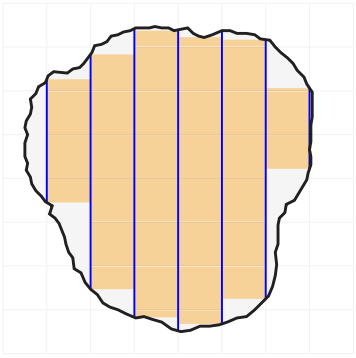

(a) Live sawing: all cuts are made in a single step at the sawmill.

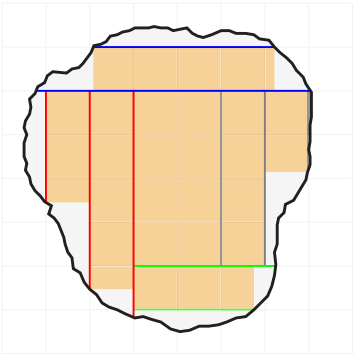

(b) Grade sawing: the blue cuts are made first, followed by rotating the log by 90° to make the red cuts, and repeating the process for the green and gray cuts, respectively.

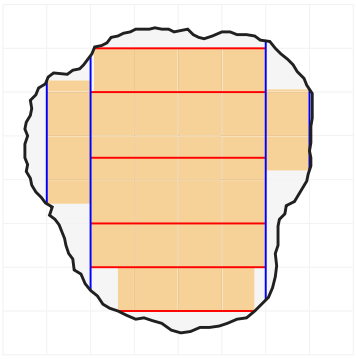

(c) Cant sawing: the blue cuts are made first, followed by rotating the log by 90° to make the red cuts.

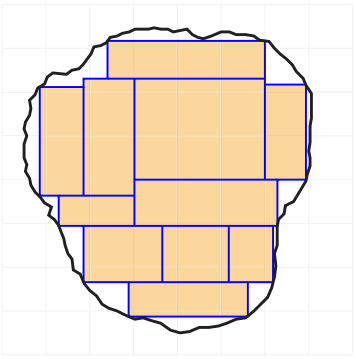

(d) Flexible sawing (used in this paper): an advanced sawmill is required due to the complexity of the cut pattern.

Fig. 1. Sawing schemes.

height. Boards are often graded based on their appearance and are used for a certain purpose, such as making furniture, flooring, and trim (Fredriksson, 2015). *Lumber*, however, refers to wooden products that are typically larger and thicker than boards and are cut to a specific thickness. Lumber is commonly graded based on strength and can be used for a wider range of purposes, such as framing, construction, and industrial applications. Optimizing for boards may require more precise cut patterns to ensure consistent quality, width, and height, while optimizing for lumber may focus more on maximizing yield and minimizing waste.

The main outcome of sawing optimization is the generation of a *cut pattern* (CP), which specifies how to cut a particular log into wooden products at a sawmill. Conventional sawmills, despite their fast processing speed, are restricted to cuts in a single direction, which limits their ability to perform complex cuts. To deal with this limitation, cut patterns must be generated based on a specific *sawing scheme* that a sawmill can execute. For instance, the live and grade sawing schemes, as shown in Figs. 1(a) and 1(b) respectively, are commonly used for lumber production, while the cant sawing scheme, shown in Fig. 1(c), is preferred for board production (Hosseini and Peer, 2022). However, restricting to one of these three sawing schemes may result in substantial material waste since the overall configuration of a cut pattern is dictated by the scheme.

One approach to minimize waste is to develop advanced sawmills that can manage more intricate cuts and offer flexible sawing schemes for CP generation, as shown in Fig. 1(d). Although such advanced sawmills are currently unavailable, the potential improvements resulting from a flexible sawing scheme may justify future technological development. The need for further research in this area is emphasized in Section 2. In this paper, we address this need by considering a flexible sawing scheme that optimizes the sawing process, aiming to maximize yield specifically for board products. For the remainder of this paper, lumber products are not considered, and the term *board* is used to refer to a board product. It is important to note that the practical feasibility of implementing flexible ways of sawing logs is mainly constrained by the limitations of conventional sawmill machinery. Nevertheless, we demonstrate a potential increase in yield, suggesting the exploration of alternative machinery for sawing logs and enabling the implementation of a flexible sawing scheme.

The remaining sections are organized as follows. Section 2 discusses the identified gap in related studies, followed by a description of the contribution made by this paper. Section 3 introduces the proposed problem and its parameters, followed by explanations of how board grading is accomplished based on wane defects. Section 4 describes the methodology applied to solve the problem. The optimization results are presented and discussed in Section 5. Finally, conclusions and directions for future work are provided in Section 6.

2. Literature review

Table 1 presents an overview of the studies reviewed in this paper from different perspectives. The following subsections will provide a detailed discussion of these studies, with an emphasis on highlighting any identified shortcomings and possible solutions to address them. For a comprehensive overview of the current state of research on

Table 1
Overview of the papers reviewed in this study.

Paper	Log geometry	Sawing scheme	CP optimization	Wane defect		Product dimensions		
				Quality criteria	Quality classes	Height	Width	Length requirements
Shevchenko et al. (2019)	Circular	Live	✓			✓		
Hinostroza et al. (2013), López and Beasley (2018), Bouzid and Salhi (2020), Silva et al. (2021, 2022) and Tole et al. (2023)	Circular	Flexible	✓			✓	✓	
Vergara et al. (2015)	Cylindrical	Not given				✓	✓	
Pradenas et al. (2013), Parra Galvez et al. (2018), Vanzetti et al. (2018) and Vanzetti et al. (2019)	Cylindrical	Cant	✓			✓	✓	
Gergel' et al. (2020)	Conic	Cant + Live	✓			✓	✓	✓
Stängle et al. (2015)	3D surface	Live				✓		
Lindner et al. (2015)	3D surface	Live				✓	✓	
Bhandarkar et al. (2002)	3D surface	Live	✓			✓		
Bommathanahalli et al. (2007) and Yun et al. (2008)	3D surface	Live	✓	✓		✓		
Thomas (2012), Morneau-Pereira et al. (2014), Rais et al. (2017) and Ursella et al. (2018)	3D surface	Cant				✓	✓	
Wessels (2009), Breinig et al. (2015) and Khaloian Sarnaghi et al. (2020)	3D surface	Cant				✓	✓	✓
Nordmark and Oja (2004), Lundahl and Grönlund (2010) and Berglund et al. (2013)	3D surface	Cant		✓	✓	✓	✓	
Fredriksson (2014)	3D surface	Cant		✓	✓	✓	✓	✓
Riesco Muñoz et al. (2013) and Fredriksson (2015)	3D surface	Cant		✓		✓	✓	✓
Correa et al. (2014)	3D surface	Cant	✓			✓		
Lin et al. (2011)	3D surface	Grade	✓			✓		
Todoroki and Rönnqvist (2002)	3D surface	Grade	✓			✓	✓	✓
Ah Shenga et al. (2015, 2016) and Shenga et al. (2017)	3D surface	Cant + Live				✓		✓
Pereira and Usenius (2006)	3D surface	Cant + Live				✓	✓	
Fredriksson et al. (2015)	3D surface	Cant + Live		✓		✓	✓	✓
Lin and Wang (2012)	3D surface	Cant + Live + Grade	✓	✓	✓	✓	✓	✓
This paper	3D surface	Flexible	✓	✓	✓	✓	✓	✓

automated decision making in wood processing, readers are referred to a survey recently published by Wery et al. (2018).

2.1. Cut pattern generation

From the perspective of CP generation in sawing optimization problems, existing studies fall into two categories: using a set of predefined CPs, and employing methods to optimize the structure of CPs as well.

2.1.1. Usage of predefined cut patterns

In studies addressing predefined CPs, a collection of CPs is created by considering sawing schemes, board specifications (i.e., height and width), and sawmill requirements (e.g., saw kerf). These CPs are then applied in the optimization problem to assign a CP to a log. For the live and cant sawing schemes, the CP assignment decision is done using two approaches. In the first approach, the CPs are selected based on the logs' top-end or butt-end diameters, see for example Nordmark and Oja (2004), Fredriksson (2014), Breinig et al. (2015) and Ah Shenga et al. (2016). In the second approach, the log is examined for all or a subset of CPs to select the one that results in a higher yield, see for example Pereira and Usenius (2006), Thomas (2012), Riesco Muñoz et al. (2013), Ursella et al. (2018) and Khaloian Sarnaghi et al. (2020).

2.1.2. Cut pattern optimization

A major drawback of using predefined CPs is that it can result in low yield. Therefore, to increase the yield some researchers attempt to optimize the log's positioning variables with respect to the generated CPs. One of these variables is the log's rotational angle, which has been investigated in Nordmark and Oja (2004), Berglund et al. (2013), Stängle et al. (2015) and Rais et al. (2017). The other important

variables, namely the parallel displacement (also known as offset) and skew of logs, are addressed in Wessels (2009), Fredriksson (2014), Ah Shenga et al. (2015, 2016) and Shenga et al. (2017).

Although studies show that optimizing these variables can increase the yield to some extent, the limitation in the number of CPs is still a major obstacle to cutting logs effectively. Another approach proposed in the literature to tackle this issue is to generate a specific CP for each log. This feature is presented under the column *CP optimization* in Table 1. As this table shows, in a majority of studies CPs are optimized considering cant, live, or grade sawing schemes.

2.2. Flexible sawing schemes

In practice, for board production, customers often demand a wide range of board sizes. For example, 80 different board types have been listed in Swedish Wood (2020). Even though cant sawing has been commonly used for board production, it is not necessarily the best approach for value optimization. One of the main reasons for this is the inherent limitation of the cant sawing scheme, as discussed earlier. Another reason is that applying a small set of predefined CPs for sawing optimization may result in low yield when dealing with boards in a wide variety of sizes. Employing a flexible sawing scheme during the CP generation process can help mitigate these challenges and lead to improved yield. The study conducted by Hinostroza et al. (2013) is an example of this kind where they formulated the sawing optimization problem as a bi-dimensional packing of rectangles in a circular container. Other similar studies include (López and Beasley, 2018; Bouzid and Salhi, 2020; Silva et al., 2021, 2022; Tole et al., 2023), which have addressed the rectangle packing problem in a similar way as Hinostroza et al. (2013). However, while these studies have optimized the rectangle packing problem from a theoretical standpoint, they may have overlooked practical considerations such as the non-cylindrical shape of real-world logs. Ignoring this factor can lead to suboptimal CPs that do not fully account for the true shape of the logs being processed.

2.3. Wane evaluation in board grading

Grading is the process of evaluating and categorizing products based on their quality and characteristics in order to determine their value. One of the most important defects involved in the grading of boards is wane, which occurs when the edge of a board lies slightly outside the surface of the log. The presence of wane in wood can negatively affect the quality of boards by reducing strength and stiffness, as well as having an impact on appearance and suitability for certain applications. There are two main methods for evaluating wane depending on the grading standards and intended use cases. One method, which can be found in Bommathanahalli et al. (2007), Yun et al. (2008), Riesco Muñoz et al. (2013), Fredriksson (2015) and Fredriksson et al. (2015), is to establish criteria to limit the amount of wane present in the boards: the column *Quality criteria* in Table 1 corresponds to this method. The other method involves assigning boards to different quality classes based on a set of rules: the column *Quality classes* in Table 1 refers to this method. Although the latter method has more practical applications, there are only a limited number of studies that have used it for board grading, see Nordmark and Oja (2004), Lundahl and Grönlund (2010), Lin and Wang (2012), Berglund et al. (2013) and Fredriksson (2014).

2.4. Research contribution

Referring to Table 1 it is seen that still no study has been conducted on value optimization with boards in the wood industry by considering a flexible sawing scheme, the log's 3D geometry, and board grading based on wane defect. Motivated by these identified gaps in the literature, this paper applies a flexible sawing scheme to maximize yield in a sawing optimization problem considering board product types and quality classes defined based on wane (see Section 3). The methodology presented in this paper consists of two phases, namely preprocessing and optimization. For the preprocessing phase, two algorithms are developed in order to generate all potential cuts considering the 3D surface of the log, the board size requirements, and the quality classes (see Section 4.1). In the first algorithm, each board is only allowed to be cut into one part across the log's length. While, in the second algorithm, dynamic programming is utilized to increase the yield by allowing each board to be cut into multiple parts across the log's length. The output of either algorithm is then fed as parameters to a maximum set packing problem (MSPP) where the objective is to obtain a feasible CP in a way that the resulting yield is maximized.

In practice, it is very important to solve a sawing optimization problem effectively in a short amount of time. To expedite the preprocessing phase, both algorithms are implemented in a system, namely FlexSaw, that utilizes parallel processing. Additionally, the FlexSaw system calls a MIP solver (CPLEX Optimizer in this paper) to solve a MSPP (see Section 4.2). The performance of the proposed methods is evaluated through a case study using the Swedish Pine Stem Bank. Furthermore, a comparison is made against the Saw2010 system (a standard tool used by researchers and Swedish sawmills) to demonstrate the advantage of flexible sawing over cant sawing.

3. Problem statement

The sawing optimization problem and board grading methods employed in this paper are discussed in the following subsections.

3.1. Problem description

Given a series of N images, taken along the length (z-axis) of a log by a CT scanner with a regular interval of $L^z = 10$ mm (in our experiments), a 3D model of the log's surface is constructed, by converting each image to a 3D slice with a thickness equal to L^z. After placing the log's model in the coordinate system and including additional margins, the design space is defined. Let W and H denote the width and height of the design space in the xy-plane, respectively.

The objective is to obtain a cut pattern (CP) that gives the maximum total value of boards, called the *value yield*. A CP is created by positioning boards within the log. The boards are selected from a set $\mathcal{T}$ of board types. For each board type t, the profile dimensions, i.e., the width w_t and height h_t of its cross-section relative to the xy-plane, are known in advance. boards can be sawed anywhere within the log as long as they satisfy specific length and quality requirements.

In this respect, two length requirements must be met: (i) the board length must be an integer multiple of a parameter called length increment, L^M, and (ii) it must not be shorter than a minimum length, denoted by L^{min}. The quality requirements are specified in terms of wane here. A set $\mathcal{Q}(t)$ of quality classes is defined for each board type t. For each quality class, the dimensions of wanes must not exceed particular thresholds: see Section 3.4. The price per unit volume of board type t under quality class q, denoted by u_{tq}, is known in advance. To generate a feasible CP, it is crucial to ensure that the boards do not overlap with each other. Also, in order to consider the thickness of the sawmill's blade, g, (known as the *saw kerf*) in the CP, there should be a minimum gap of g between sawed boards.

3.2. Notation

The notation given in Table 2 is used throughout this paper to define board types, quality classes, and important parameters (others are listed in Appendix A and will be discussed later on):

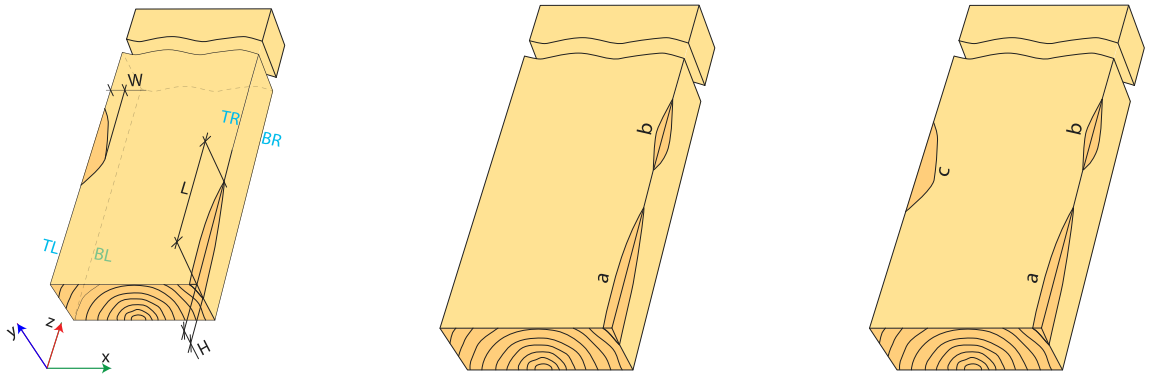

(a) The four (of twelve) edges of the four (of six) faces of a board that are examined for wane (namely top-left (TL), top-right (TR), bottom-left (BL), and bottom-right (BR)), along with the dimensions of wane (namely width (W), height (H), and length (L)).

(b) Example of edge wane.

(c) Example off ace wane.

Fig. 2. Illustration of wane parameters and their types.
Image source: Swedish Wood (2020).

3.3. Quality checking

In this paper we focus on wane as the type of defect that can affect the quality of sawed boards, following the standard established by Swedish Wood (2020). However, the quality checking introduced here can be extended to cover other types of defects, provided they can be expressed mathematically. Each board is intersected with the log's surface in order to measure the dimensions of its wanes, namely width (W), height (H), and length (L), as shown in Fig. 2(a). Wane is only considered on four edges, designated in Fig. 2(a). If wane appears on only one of those edges, then the resulting defect is called *edge wane*, otherwise, if they appear on the two edges of a face, then the resulting defect is called *face wane*. Note that wane on edges of distinct faces or on more than two edges is not permissible.

There are four parameters, $(W^{\max}, H^{\max}, LE^{\max}, LF^{\max})$, for each board type and quality class that must be adhered to in order to limit the size of wanes. The parameters $W^{\max}$ and $H^{\max}$ respectively specify the maximum width and height of each individual wane. The parameters $LE^{\max}$ and $LF^{\max}$ respectively specify the maximum cumulative length of edge and face wanes, and both are represented as a percentage of the board length. For example, in Fig. 2(b), the sum $L_a + L_b$ must not exceed $\ell \cdot LE^{\max}/100$, where ℓ denotes the length of the board. Similarly, as per Fig. 2(c), the sum $L_a + L_b + L_c$ must not exceed $\ell \cdot LF^{\max}/100$.

Determine whether a board of type t meets the wane requirements for quality class q if it is cut at the placement $(x, y, z^{\mathrm{s}}, z^{\mathrm{e}})$ within the log corresponds to a Boolean function. The notation IsValid$(t, q, x, y, z^{\mathrm{s}}, z^{\mathrm{e}})$ is used to denote this Boolean function. The coordinates (x, y) correspond to the bottom-left corner of the board's profile on the xy-plane, and z^{s} and z^{e} are the starting and ending slices of the log where the board is placed (note that we must have $z^{\mathrm{s}}, z^{\mathrm{e}} \in \{1, 2, \ldots, N\}$ and $z^{\mathrm{e}} \geq z^{\mathrm{s}}$). The function IsValid returns **true** if such a board meets the wane requirements and **false** otherwise. The code for IsValid is not provided here as the explanations above are sufficient to reconstruct it.

3.4. Board grading

To determine the value of a potential board, the function Grade(t, x, y, z_0, z_1) is used. Its arguments are the board type, t, the x- and y-coordinates where the bottom-left corner of the profile of such a board is placed, (x, y), and the starting and ending slices of the log where the board can be placed, z_0 and z_1. The function begins by initializing the best value of the board, v^*, to zero. Then, for each quality class $q \in Q(t)$, the function applies a greedy approach to identify an interval $[z, z + \ell - 1]$ within $[z_0, z_1]$ for placing the board. The variables z and ℓ respectively represent the starting slice of the interval and the consecutive count of valid slices in the interval. These variables are initialized in Lines 3 and 4. As long as the condition $z + \ell \leq z_1$ is satisfied, the function checks three cases between Lines 5 and 13. If IsValid$(t, q, x, y, z, z + \ell)$ holds, ℓ is incremented by one in Line 7, otherwise if still, ℓ is zero, z is incremented by one in Line 9, and if none of those two cases are met, i.e. IsValid$(t, q, x, y, z, z + \ell)$ does not hold and $\ell \geq 1$, there is no point in trying longer lengths as they are also invalid, by definition. In this case, v^* is updated in Line 12 if the length requirements are met in Line 11, and the algorithm breaks from the while loop. The function is considered greedy because, to reduce the computational time, it does not exhaustively search for all possible intervals within the range $[z_0, z_1]$.

Table 2
Main notation used in this paper.

Sets:	
$\mathcal{T}$	Set of board types
$Q(t)$	Set of quality classes for a board of type $t \in \mathcal{T}$
Indices:	
z, z_0, z_1	Index of slices of the log
t, t'	Index of board types
q	Index of quality classes
Parameters:	
N	Number of slices of the log
W	Horizontal boundary of the log in the x-axis (width of the design space)
H	Vertical boundary of the log in the y-axis (height of the design space)
L^{z}	Thickness of each slice of the log
g	Saw kerf (thickness of the sawmill's blade)
w_t	Profile width of board type $t \in \mathcal{T}$
h_t	Profile height of board type $t \in \mathcal{T}$
u_{tq}	Unit price of board type $t \in \mathcal{T}$ of quality class $q \in Q(t)$ per unit volume
$L^{\min}$	Minimum length of boards, $L^{\min} \geq L^{\mathrm{z}}$
L^{M}	Length increment of boards

Function Grade(t, x, y, z_0, z_1)

```
1  v* ← 0
2  foreach q ∈ Q(t) do
3      z ← z_0
4      ℓ ← 0
5      while z + ℓ ≤ z_1 do
6          if IsValid(t, q, x, y, z, z + ℓ) then
7              ℓ ← ℓ + 1 // ℓ is the consecutive count of valid
                 slices in the interval
8          else if ℓ = 0 then
9              z ← z + 1 // z is the starting slice of the interval
10         else
11             if ℓ · L^z ≥ L^min and ℓ · L^z mod L^M = 0 then
12                 v* ← max{v*, u_tq · w_t · h_t · ℓ · L^z}
13             break
14 return v*
```

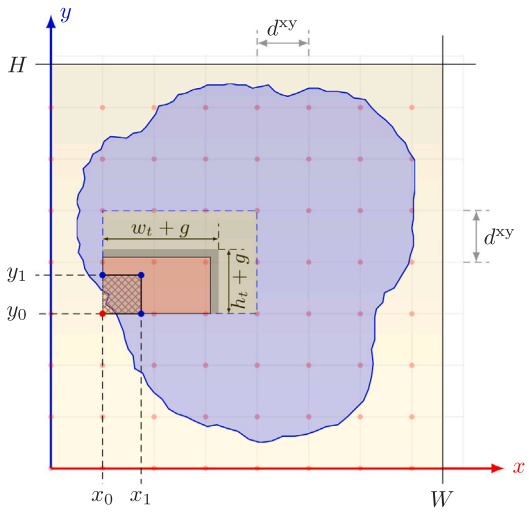

Fig. 3. Possible points evaluated by function 4PointsGrade. In the figure, $d^{xy} \times d^{xy}$ is the pixel size and each red dot corresponds to the lower-left corner of a pixel.

Function 4PointsGrade(t, i, j, z_0, z_1)

```
1  (x_0, y_0) ← (i · d^xy, j · d^xy)
2  (x_1, y_1) ← (x_0 + ⌈(w_t + g)/d^xy⌉ d^xy − w_t − g, y_0 + ⌈(h_t + g)/d^xy⌉ d^xy − h_t − g)
3  return max_{x∈{x_0,x_1}, y∈{y_0,y_1}} {Grade(t, x, y, z_0, z_1)}
```

4. Solution methods

This paper proposes two solution methods for the sawing optimization problem, called the 2D and 2D+ sawing methods. Both sawing methods consist of two steps: a preprocessing step followed by solving a maximum set packing problem (MSPP) to obtain a CP based on the flexible sawing scheme. Section 4.1 provides detailed explanations of these steps and Section 4.2 introduces the developed FlexSaw system that implements the proposed methods.

4.1. Preprocessing and solving

The aim of preprocessing is to generate potential sawing positions by discretizing the design space into pixels (not to be mixed up with the pixels of a CT scan image) and evaluating the possible placements of all board types using those pixels. To do so, the xy-plane is partitioned into pixels using a set of equally-spaced horizontal and vertical lines. Let d^{xy} denote the distance between two consecutive vertical or horizontal lines so that each pixel is of dimension $d^{xy} \times d^{xy}$: see Fig. 3 for an illustration. Using the notations defined in Table 2, the set of pixel indices (just called pixels from now on) is $\mathcal{P} = \left\{(i,j) \in \mathbb{N}_0^2 \mid i < \frac{W}{d^{xy}},\ j < \frac{H}{d^{xy}}\right\}$.

A simple way to position the lower-left corner of a potential board on a specific pixel (i, j) is to compute the coordinates of the lower-left corner of the board's profile as $(x, y) = (i \cdot d^{xy}, j \cdot d^{xy})$. However, this yields only one possible point for each pixel (i, j), limiting the potential sawing positions for large values of d^{xy}. One idea to explore more sawing positions without sacrificing too much time is to consider the corner points of the rectangle defined by $x \in [x_0, x_1]$ and $y \in [y_0, y_1]$ for the placement of the lower-left corner of the board's profile, where $x_0 = i \cdot d^{xy}$, $y_0 = j \cdot d^{xy}$, $x_1 = x_0 + \left\lceil \frac{w_t+g}{d^{xy}} \right\rceil d^{xy} - w_t - g$, and $y_1 = y_0 + \left\lceil \frac{h_t+g}{d^{xy}} \right\rceil d^{xy} - h_t - g$. The corresponding rectangle is highlighted with cross-hatched lines in Fig. 3. As this figure also shows, the board with the red profile overlaps with the pixels within the region enclosed by the dashed border even if its lower-left corner is placed on any of the other three corner points of that rectangle, indicated by the blue dots. The function 4PointsGrade(t, i, j, z_0, z_1) takes board type, t, pixel, (i, j), and starting and ending slices of the log where such a board can be placed, (z_0, z_1), as arguments and returns the best value obtained by calling Grade for the four corner points.

A summary of the notation used in the 2D and 2D+ sawing methods is given in Table A.1 in Appendix A. Procedure Initialize, given in Appendix B, is employed to initialize the necessary sets for the respective sawing method. Detailed explanations of the sawing methods and associated notation are presented in Sections 4.1.1 and 4.1.2.

4.1.1. The 2D sawing method

The pseudo-code of the 2D sawing method is given in Algorithm 1. For any pixel $u = (i, j) \in \mathcal{P}$, the value of a board of type t, denoted v_{tp}, is obtained in Line 5 assuming that the board can only be sawed between the first and last slices of the log, i.e., $z_0 = 1$ and $z_1 = N$. If v_{tp} is positive, then the pair (t, p) is called a *configuration* and is considered an alternative for the optimization problem. Unnecessary configurations are eliminated by setting $v_{tp} = 0$ if $v_{t'p} \le v_{tp}$ and $\Pi' \subseteq \Pi$, where Π' is the set of pixels overlapped by a board of type t' placed at p and Π is the set of pixels overlapped by a board of type t placed at p. This elimination process is done through Lines 6 to 10. Let the set $\mathcal{I}(t)$ denote the pixels where a board of type t can be sawed and $S(p)$ denote the set of configurations overlapping with pixel p. If v_{tp} remains positive after the elimination process, pixel p is added to $\mathcal{I}(t)$ in Line 11. Also, from Lines 12 to 15, (t, p) is added to $S(p')$ for each pixel p' that overlaps with the corresponding configuration. The preprocessing step in Lines 1 to 16 may take considerable time if d^{xy} is chosen to be relatively small. The computations within the outer loop of Algorithm 1 for each $p \in \mathcal{P}$ are highly independent, and parallel processing can be utilized by implementing that loop on multiple threads.

Once the preprocessing step is completed, a MSPP is solved in Line 17 to obtain a CP. The binary decision variable x_{tp} is introduced to represent whether the CP includes the configuration (t, p) or not. The MSPP is formulated as the following mathematical model:

$$\text{(2D Sawing)} \quad \text{maximize} \quad \sum_{t \in \mathcal{T}} \sum_{p \in \mathcal{I}(t)} v_{tp} x_{tp} \tag{1a}$$

$$\text{subject to} \quad \sum_{t \in S(p)} x_{tp} \le 1, \quad \forall p \in \mathcal{P}, \quad |S(p)| \ge 2, \tag{1b}$$

$$x_{tp} \in \{0, 1\}, \quad \forall t \in \mathcal{T}, \quad p \in \mathcal{I}(t). \tag{1c}$$

The objective function (1a) maximizes the value of the boards in the CP. The constraints (1b) ensures the selection of at most one configuration among those that overlap with a pixel, and the constraints (1c) ensures that the decision variables can only be 0 or 1.

Algorithm 1: 2D sawing

Result: $\boldsymbol{x}$

1 Initialize(2D Sawing)
2 **parfor** $p \in \mathcal{P}$ **do**
3 $(i, j) \leftarrow p$
4 **foreach** $t \in \mathcal{T}$ **do**
5 $v_{tp} \leftarrow$ 4PointsGrade$(t, i, j, 1, N)$
6 **foreach** $t \in \mathcal{T} : v_{tp} > 0$ **do**
7 **foreach** $t' \in \mathcal{T} \setminus \{t\}$ **do**
8 **if** $\left\lceil \frac{w_{t'}+g}{d^{xy}} \right\rceil \le \left\lceil \frac{w_t+g}{d^{xy}} \right\rceil$ **and** $\left\lceil \frac{h_{t'}+g}{d^{xy}} \right\rceil \le \left\lceil \frac{h_t+g}{d^{xy}} \right\rceil$ **and** $v_{tp} \le v_{t'p}$ **then**
9 $v_{tp} \leftarrow 0$
10 **go to** next
11 $\mathcal{I}(t) \leftarrow \mathcal{I}(t) \cup \{p\}$
12 **foreach** $p' \in \mathcal{P}$ **do**
13 $(i', j') \leftarrow p'$
14 **if** $i \le i' < i + \frac{w_t+g}{d^{xy}}$ **and** $j \le j' < j + \frac{h_t+g}{d^{xy}}$ **then**
15 $\mathcal{S}(p') \leftarrow \mathcal{S}(p') \cup \{(t, p)\}$
16 next :
17 **solve** 2D Sawing **using** MIP solver and **return** $\boldsymbol{x}$

Procedure DPEval$(\boldsymbol{v}^+, p)$

1 $(i, j) \leftarrow p$
2 **foreach** $b \in \mathcal{B}$ **do**
3 **foreach** $c \in C$ **do**
4 $(k, k') \leftarrow c$
5 $v'_{bc} \leftarrow \max_{t \in \mathcal{T}^+(b)} \left\{ \text{4PointsGrade}(t, i, j, z^0_k, z^1_{k'}) \right\}$
6 $v'_{bc} \leftarrow \max_{b'=(m',n')} \left\{ v'_{b'c} \mid (m, n) = b,\ m' \in \{m, m-1\},\ n' \in \{n, n-1\},\ m', n' \ge 1 \right\}$
7 $v^*_{0,k} \leftarrow 0,\ \forall k \in \mathcal{K}$
8 **for** $s \leftarrow 1$ **to** M **do**
9 **for** $k \in \mathcal{K} : k \ge s$ **do**
10 $v^*_{sk} \leftarrow \max_{\substack{k' \in \mathcal{K} \\ k' < k}} \left\{ v^*_{s-1,k'} + v'_{b,(k'+1,k)} \right\}$
11 $v^+_{pb} \leftarrow \max_{s \in \{1,\dots,M\}} \left\{ v^*_{s,|\mathcal{K}|} \right\}$
12 **foreach** $b \in \mathcal{B} : v^+_{pb} > 0$ **do**
13 $(m, n) \leftarrow b$
14 **for** $m' \leftarrow 1$ **to** m **do**
15 **for** $n' \leftarrow 1$ **to** n **do**
16 $b' \leftarrow (m', n')$
17 **if** $m' \ne m$ **or** $n' \ne n$ **and** $v^+_{pb'} \ge v^+_{pb}$ **then**
18 $v^+_{pb} \leftarrow 0$
19 **go to** next
20 next :

Algorithm 2: 2D+ sawing

Result: $\boldsymbol{x}^+$

1 Initialize(2D+ Sawing)
2 **parfor** $p \in \mathcal{P}$ **do**
3 $(i, j) \leftarrow p$
4 DPEval$(\boldsymbol{v}^+, p)$
5 **foreach** $b \in \mathcal{B} : v^+_{pb} > 0$ **do**
6 $\mathcal{I}^+(p) \leftarrow \mathcal{I}^+(p) \cup \{b\}$
7 **for** $i' \leftarrow i$ **to** $i + m - 1$ **do**
8 **for** $j' \leftarrow j$ **to** $j + n - 1$ **do**
9 $p' \leftarrow (i', j')$
10 $\mathcal{S}^+(p') \leftarrow \mathcal{S}^+(p') \cup \{(p, b)\}$
11 **solve** 2D+ Sawing **using** MIP solver and **return** $\boldsymbol{x}^+$

4.1.2. The 2D+ sawing method

The 2D sawing method described in Section 4.1.1 only allows boards to be examined for one starting and ending slice of the log, limiting the effectiveness of the method on a log with a highly irregular shape or pith. To address this limitation, the 2D sawing method is extended to allow the examination of multiple starting and ending slices across the z-axis. In the extended method, called the *2D+ sawing method*, board types fitting into the same number of horizontal and vertical pixels are grouped into what we call a *block*. Let (m, n) denote a block of size $m \times n$, where m and n are the numbers of horizontal and vertical pixels in the block, respectively. The set of possible block sizes is denoted by $\mathcal{B}$ and is defined using procedure Initialize in Line 7 (in Appendix B). For every block $b \in \mathcal{B}$, the set $\mathcal{T}^+(b)$, defined in Line 8, denotes the board types that only fit into b; in other words, the set $\mathcal{T}$ is partitioned into sets $\mathcal{T}^+(b)$.

In order to examine multiple starting and ending slices for sawing boards, the slices of the log are divided into a set of equally long segments, each of length d^z. The set $\mathcal{K}$ of segments is defined in Line 9. For each segment $k \in \mathcal{K}$, its starting and ending slices on the log, denoted z^0_k and z^1_k, are calculated in Lines 10 and 11, respectively. The set C, defined in Line 12, represents all segment pairs $(k, k') \in \mathcal{K}^2$ that meet the requirement on minimum board length. A DP algorithm, given by procedure DPEval$(\boldsymbol{v}^+, p)$, is utilized to determine the optimal segmentation for every block size positioned on pixel p and update some of the v^+_{pb} values within the vector $\boldsymbol{v}^+$. Each local variable v'_{bc} denotes the value of block b within segmentation $(k, k') = c \in C$; it is calculated in Line 5. Subsequently, the optimal segmentation for a block of size b is obtained recursively in M stages (M is initialized in Line 13 of procedure Initialize in Appendix B) in Lines 7 to 10, where v^*_{sk} is a local variable that stores the best value at stage s up to segment k. Finally, the value of a block of size b at pixel p, denoted by v^+_{pb}, is determined in Line 11. The second part of the algorithm, given in Lines 12 to 20, decreases the number of configurations (p, b) by setting $v^+_{pb} = 0$ if there exists a smaller block size with at least the same value as v^+_{pb}.

For each pixel $p \in \mathcal{P}$, Algorithm 2 computes all v^+_{pb} values in Line 4 using the DP algorithm. After that, sets $\mathcal{I}^+(p)$ and $\mathcal{S}^+(p)$ are updated accordingly in Lines 6 and 10, where $\mathcal{I}^+(p)$ is the set of pixels where a block of size b can be sawed, and $\mathcal{S}^+(p)$ is the set of pairs (p', b) overlapping with pixel p (these two sets are later used in a MSPP). Since the outer loop of the algorithm, Lines 2 to 10, is highly separable, it is possible to distribute computations across multiple threads and reduce the preprocessing time. Once the preprocessing step is completed, a MSPP is solved in Line 11 to obtain a CP. The binary decision variable x^+_{pb} is used to decide whether the CP includes the configuration (p, b) or not. The corresponding MSPP is represented by the following mathematical model:

$$\text{(2D+ Sawing)} \quad \text{maximize} \quad \sum_{p \in \mathcal{P}} \sum_{b \in \mathcal{I}^+(p)} v^+_{pb} x^+_{pb} \tag{2a}$$

$$\text{subject to} \quad \sum_{(p', b) \in \mathcal{S}^+(p)} x^+_{p'b} \le 1, \quad \forall p \in \mathcal{P}, \quad \left|\mathcal{S}^+(p)\right| \ge 2, \tag{2b}$$

$$x^+_{pb} \in \{0, 1\}, \quad \forall p \in \mathcal{P}, \quad b \in \mathcal{I}^+(p). \tag{2c}$$

The objective function defined by (2a) maximizes the value yield of the resulting CP, the constraints (2b) ensures no overlap occurs between the blocks, and the constraints (2c) ensures that the decision variables can only be 0 or 1.

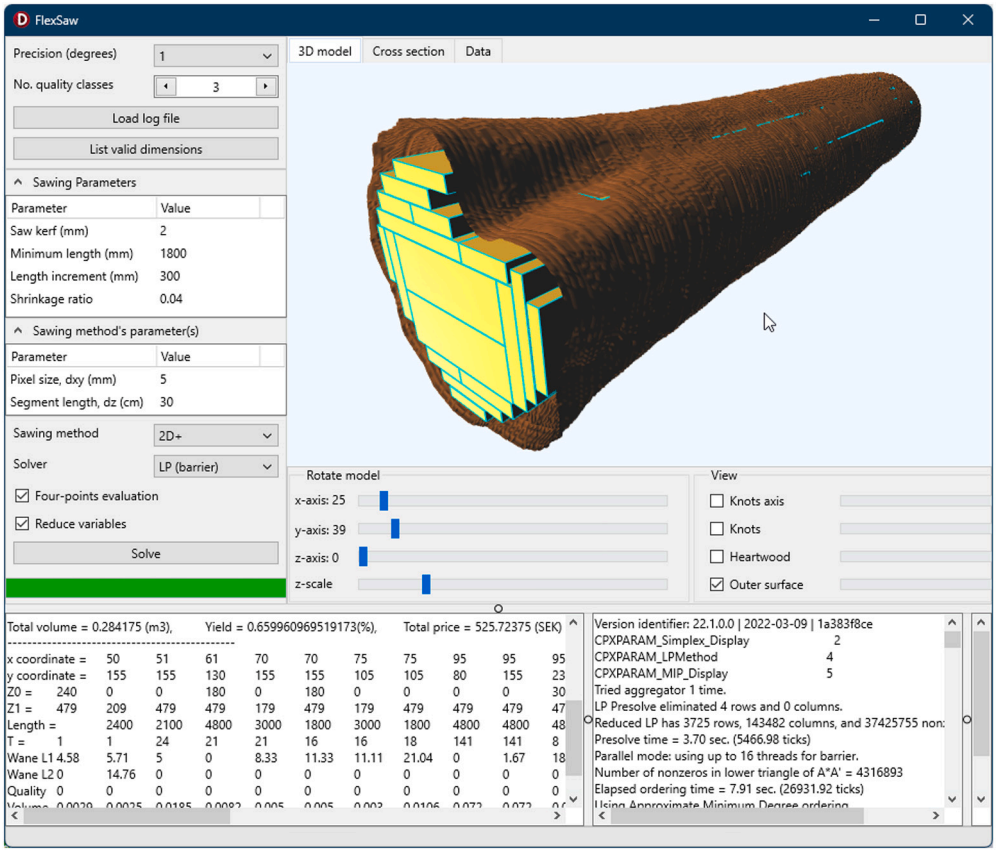

Fig. 4. User interface of the developed FlexSaw system.

4.2. Developed system

The implementation of the 2D and 2D+ sawing methods resulted in a system, namely FlexSaw, developed using RAD Studio 11.2. It is important to mention that the actual implementation of the proposed algorithms differs slightly from what is described in this paper: certain variables, such as the type, quality class, length, and coordinates of each product in the CP, need to be tracked in order to reconstruct the solution after solving the MSPPs. However, these details were omitted from the pseudo-code to simplify the discussion.

FlexSaw allows the loading of logs from the Swedish Pine Stem Bank (Grönlund et al., 1995), selecting board profiles, and setting parameters such as saw kerf and minimum board length. General quality classes for wane requirements can be defined in one place for all boards, but individual modifications can be made for each board type and quality class afterward. FlexSaw takes advantage of parallel processing to speed up preprocessing and is linked to the IBM CPLEX 22.1 optimizer to solve the generated MSPP. Once solved, FlexSaw displays a 3D and 2D view of the obtained CP within the log and generates a detailed report including the exact sawing position, value, and quality class of each board, as well as the preprocessing and solution times. The user interface of FlexSaw is shown in Fig. 4.

5. Experiments

Instances were solved using our FlexSaw system to evaluate the effectiveness of the 2D and 2D+ sawing methods. The computations were conducted on a machine with an x64 Windows 10 operating system, featuring an Intel Core i9-11900K processor (with 8 cores and 16 threads), and 64 GB of RAM. The descriptions of the benchmark data are given in Section 5.1. In Section 5.2, the proposed sawing methods were compared against an existing tool that applies a cant sawing scheme. Sensitivity analyses were carried out in Sections 5.3 and 5.4 to investigate the effect of different d^{xy} and d^{z} values on the performance of the proposed sawing methods. Finally, the effect of saw kerf on the yield is investigated in Section 5.5.

5.1. Benchmark data

Fifty-nine sample logs from the Swedish Pine Stem Bank (Grönlund et al., 1995) are used for benchmarking. The benchmark consists of the first three sets of scanned data of the Stem Bank, covering different log diameters from different areas in Sweden. Each set is called a *plot* and contains six trees. The trees, depending on their length, were cut into two to four logs, resulting in a total of 59 logs. The outer shape of the logs and their internal properties were recorded using a medical CT scanner. The characteristics of the logs are provided in Table 3.

The board types used in the experiments adhere to the Swedish Wood (2020) standard. Fig. 5 shows the 80 board types and their nominal profile dimensions. To ensure that the final boards meet the standard after undergoing the drying process, the nominal dimensions are to be multiplied by $(1 + \alpha)$ and rounded up, where α represents the shrinkage ratio in the width and height of a board and is assumed to be 0.04; shrinkage in the length of a board is assumed to be negligible. In order to enable a CP to accommodate both horizontal and vertical versions of the same board type, two variations of each profile dimension are included in the set of board types: one for horizontal orientation and one for vertical orientation (achieved by swapping its width and height). The two square-shaped board profiles are only considered once. As a result, there are a total of 158 board types to be examined in the experiments.

As for the other parameters, the saw kerf g, the minimum board length $L^{\min}$, and the length increment L^{M} are set to 2 mm, 1800 mm, and 300 mm, respectively (Fredriksson, 2014). The grading rules for

Table 3
Characteristics of the logs selected from the Swedish Pine Stem Bank, as well as the baseline optimization results of value yield obtained using the SAW2010 program. One Swedish krona (SEK) is about 10% of a euro.

Instance number	Plot	Tree	Log	Top diameter (mm)	Bottom diameter (mm)	Length (mm)	Value yield (SEK)	Instance number	Plot	Tree	Log	Top diameter (mm)	Bottom diameter (mm)	Length (mm)	Value yield (SEK)
1	1	1	1	151.1	203.7	4480	81.5	31	2	5	3	205.7	265	4970	213.6
2	1	1	2	129.7	155.3	4540	68.1	32	2	6	1	312.3	373.4	4210	435.1
3	1	2	1	157.8	197.6	4420	89.9	33	2	6	2	283.6	317.5	4190	332.2
4	1	2	2	130.1	161.3	4110	66.3	34	2	6	3	259	285.3	4270	290.6
5	1	3	1	167.5	224.9	4580	124.5	35	2	6	4	217.5	257.8	4710	213.6
6	1	3	2	138.7	167.8	4550	86.3	36	3	1	1	289.9	351.3	4900	417.9
7	1	4	1	165.3	218.4	5080	128.9	37	3	1	2	257.7	287.2	5010	366.5
8	1	4	2	132.2	167.1	4970	84.6	38	3	1	3	229	259.7	4410	228.6
9	1	5	1	200.1	253.3	4400	174.4	39	3	1	4	189.5	226.2	3670	122.1
10	1	5	2	200.7	170.9	4530	106.8	40	3	2	1	295.1	342.7	4830	399.0
11	1	5	3	131.6	170.6	4140	70.4	41	3	2	2	252.3	283.4	4340	297.8
12	1	6	1	187.5	232.4	4830	154.0	42	3	2	3	211.8	252.8	4350	203.9
13	1	6	2	164.6	189.5	3790	101.2	43	3	2	4	169.6	214.7	4220	89.4
14	1	6	3	131	164.7	4170	74.3	44	3	3	1	315.9	369.8	4990	513.3
15	2	1	1	223.3	282.4	4340	209.8	45	3	3	2	284.6	311.8	4800	392.9
16	2	1	2	227.3	249.9	4170	209.4	46	3	3	3	243.2	285.7	4960	316.3
17	2	1	3	203.4	221.8	4200	160.3	47	3	3	4	199.4	240.9	4020	163.2
18	2	1	4	175.5	198.2	3450	90.8	48	3	4	1	314.1	411.1	4770	497.1
19	2	2	1	231.9	294.7	4930	262.9	49	3	4	2	284.4	312.6	3970	328.9
20	2	2	2	203.4	237.6	4580	196.3	50	3	4	3	244.6	291.7	4410	287.2
21	2	2	3	168.2	205.7	4050	112.7	51	3	4	4	198.3	247.5	4380	180.5
22	2	3	1	267	333.1	4800	314.0	52	3	5	1	317.5	390.8	4980	509.1
23	2	3	2	239	272.9	4670	278.4	53	3	5	2	293.4	318.3	4940	415.3
24	2	3	3	201.9	241.7	4830	193.0	54	3	5	3	247	299.5	4810	303.0
25	2	4	1	271.6	348	4290	291.3	55	3	5	4	200.7	245.1	4130	157.2
26	2	4	2	246	279	4620	292.4	56	3	6	1	336.4	425.6	5010	605.6
27	2	4	3	213.2	248.2	3950	172.6	57	3	6	2	299.9	333.9	4860	431.4
28	2	4	4	174.4	217.9	4000	124.5	58	3	6	3	259.6	298.1	4650	305.1
29	2	5	1	294.8	369.6	4780	432.0	59	3	6	4	206.4	258.2	5040	192.3
30	2	5	2	257.7	300	5020	342.8								

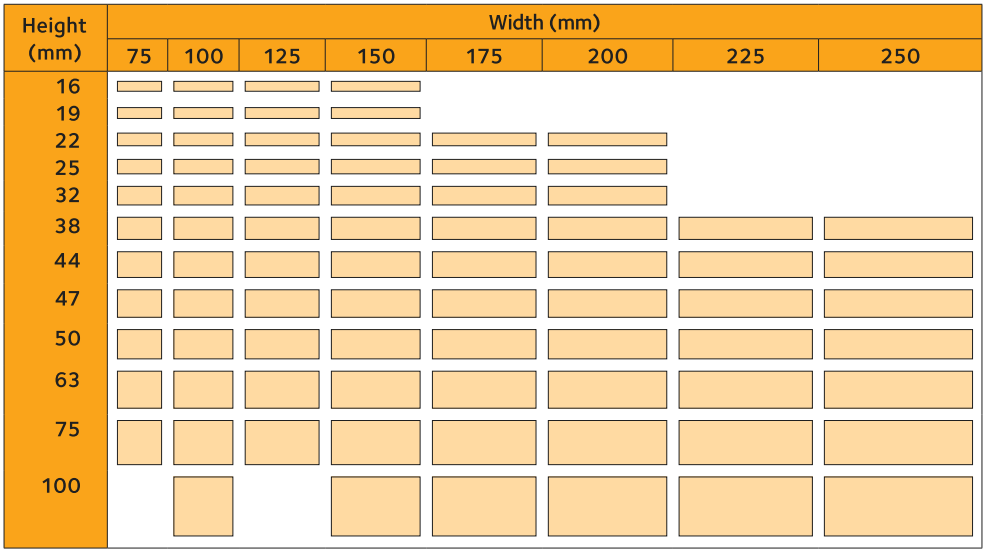

Fig. 5. Nominal profile dimension of the board types considered in the experiments.
Image source: Swedish Wood (2020).

assessing the quality of sawed boards with respect to wane are adopted from Nordmark and Oja (2004), Fredriksson (2012) and Johansson (2013) and are presented in Table 4. There are three quality classes: OS, V, and VI. The second and third columns of Table 4 provide the maximum cumulative width and height of the wanes for each quality class. The fourth and fifth columns specify the maximum total lengths (in percent) of the edge and face wanes for each quality class (see Section 3.3 for more details). The last column indicates the unit price of boards in SEK/m^3 for each quality class (Fredriksson, 2012).

5.2. Computational results

A pixel size of $d^{xy} = 5$ mm was used for both the 2D and the 2D+ sawing methods. The 2D+ sawing method was executed for segment sizes of 20 cm, 30 cm, 40 cm, and 50 cm, and the best result was

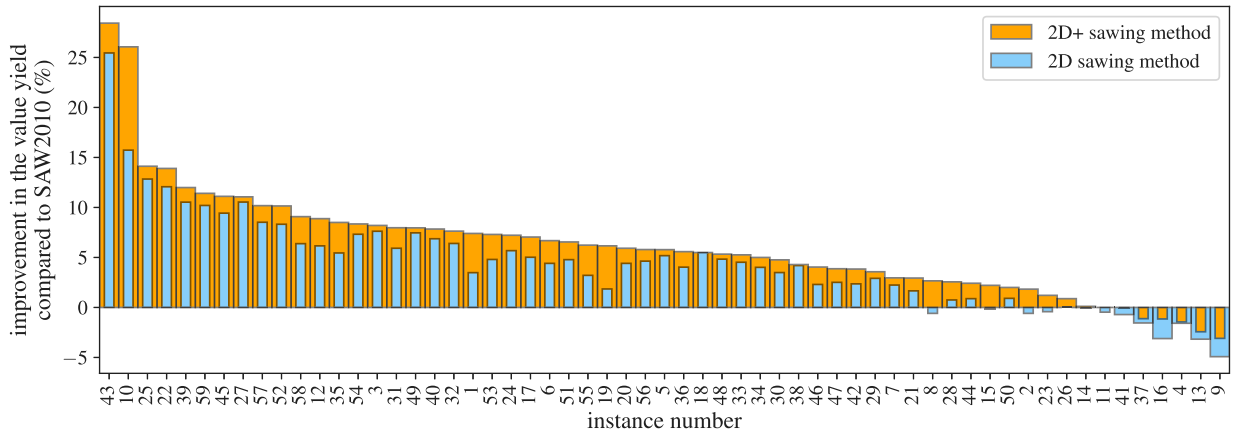

Fig. 6. Improvement achieved using the 2D and 2D+ sawing methods compared to the baseline in Table 3 by the SAW2010 system.

Table 4
Quality classes employed in the experiments for grading products based on wane.

Quality class	Wane limitation parameters (see Section 3.3)				Price (SEK/m^3)
	$W^{\max}$ (mm)	$H^{\max}$ (mm)	$LE^{\max}$ (%)	$LF^{\max}$ (%)	
OS	5	7	30	20	1850
V	5	10	30	20	1600
VI	25	15	50	40	1000

taken (assuming that each test can be done in parallel on separate machines). To demonstrate the potential benefits of the proposed sawing methods, a comparison was made against an existing tool that is capable of reading the Stem Bank data. The tool, called SAW2010, is an evolved version of the SAW2003 system developed by Nordmark (2005). Designed specifically for conventional sawmills, SAW2010 utilizes simulation techniques to choose the CP resulting in the highest value yield from a range of options that are generated based on the cant sawing scheme. To ensure comparability of the results, SAW2010 was configured to exclude features that were not taken into account in this study, such as knots. The value yield obtained by SAW2010 is in Table 3.

Fig. 6 presents the potential improvement achievable by our proposed sawing methods compared to SAW2010. Out of 59 logs, the 2D and 2D+ sawing methods obtained better solutions for 48 and 53 logs respectively. By our two methods, the total value yield of the 59 logs is about 14,959 SEK and 15,177 SEK respectively, resulting in 4.59% and 6.11% improvements compared to SAW2010, which gives about 14,302 SEK. While the practical implementation of a flexible sawing scheme faces challenges in today's sawmills due to the limitation of sawmill machinery, the potential increase in value yield promotes the exploration of alternative machinery for log disintegration that enable the adoption of the proposed flexible sawing scheme.

According to Fig. 6, the 2D and 2D+ sawing methods can improve the value yield by up to 25.5% and 28.4%, respectively (which corresponds to log 43). Log 10 stands out with the second highest improvement. Interestingly, this log also corresponds to the largest deviation between the 2D and 2D+ sawing methods. For this particular log, the obtained solutions are depicted in Fig. 7. As this figure shows, the key difference between the 2D and 2D+ methods is the 2D+ capability for the placement of multiple boards across a log's length, resulting in a higher value yield.

To highlight the differences among the three sawing methods we apply the *performance profiles* tool which was developed by Dolan and Moré (2002) for evaluating and comparing the performance of optimization algorithms. We consider the value yield as a performance measure and define the *performance ratio* of a sawing method on log x using $r_x = \frac{V_x^{\max}}{V_x}$, where $V_x^{\max}$ is the best value yield by any sawing tool on log x, and V_x is the value yield of a sawing tool on log x. Fig. 8 shows the performance profiles for the 2D and 2D+ sawing methods, as well as SAW2010 system. For each value of $\tau \in \mathbb{R}$ on the horizontal axis, the vertical axis reports the fraction of logs for which the performance ratio of the corresponding sawing tool is at most τ, i.e., $\rho(\tau) = \frac{1}{59}\text{size}\{r_a \leq \tau\}$. In the performance profile, the best performance is achieved by those algorithms whose curves appear highest in the chart, "wrapping" the other curves. As Fig. 8 shows, the best performance is achieved by the 2D+ sawing method as its performance profile appears highest in the chart. In about 90% of the logs (see the left most of the figure at $\tau = 1$), the 2D+ sawing method was able to achieve the best performance ratio. At $\tau = 1$, SAW2010 is the second-best performer, followed by the 2D sawing method. Although, for a very small slope of the horizontal axis, i.e., $\tau \leq 1.0054$, SAW2010 dominates the 2D sawing method, for the majority of the horizontal axis the 2D sawing method dominates SAW2010.

5.3. Sensitivity analysis of the 2D sawing method

To examine how the performance of the 2D sawing method is affected by the pixel size d^{xy}, the instances were studied with two other pixel sizes, namely 10 mm and 20 mm. As previously mentioned, out of the 59 logs, better solutions are obtained for 48 logs when $d^{\text{xy}} = 5$ mm, compared to SAW2010. For $d^{\text{xy}} = 10$ mm and $d^{\text{xy}} = 20$ mm, this number decreases to 37 and 23 logs, respectively. With $d^{\text{xy}} = 10$ mm, the total value yield of the logs is about 14,633 SEK, still indicating an improvement of 2.31%. However, with $d^{\text{xy}} = 20$ mm, the 2D sawing method cannot compete with SAW2010: the total value yield is approximately 14,261 SEK, which is about 0.29% worse than that with SAW2010.

While using a 5 mm pixel size produces the best results, it comes with a significant increase in solution time (excluding the preprocessing time) for logs with larger diameters. For example, log 56 takes over 100 s to solve with $d^{\text{xy}} = 5$ mm, while the time is less than four seconds with $d^{\text{xy}} = 10$ mm. As seen in Fig. 9, for $d^{\text{xy}} = 5$ mm, the number of binary variables and constraints grows much more rapidly as the average diameter of a log (the average of its top and bottom diameters, given in Table 3) increases, resulting in a longer solution time. Fig. 10 compares $d^{\text{xy}} = 10$ mm and $d^{\text{xy}} = 20$ mm against $d^{\text{xy}} = 5$ mm in terms of the relative gap between the value yields: it shows that the relative gaps reduce as the log diameter increases. Therefore, if a shorter computation time (defined as the sum of the preprocessing time and the solution time) is desired, then a 10 mm pixel size can be used for larger logs.

The effect of using the 4PointsGrade evaluation function is another important aspect. To examine this, the instances are solved once again

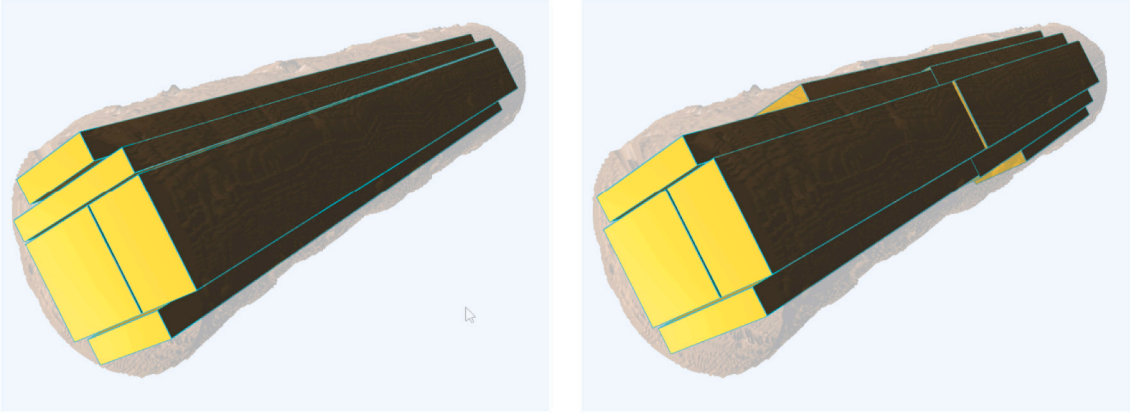

(a) 2D sawing method with a value yield of 123.55 SEK.

(b) 2D+ sawing method with a sawing value of 134.58 SEK.

Fig. 7. Comparison of the solutions obtained for log 10 using the proposed sawing methods.

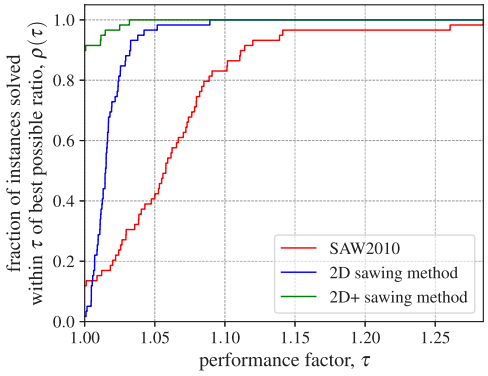

Fig. 8. Performance profile of the sawing tools over the entire dataset of 59 logs.

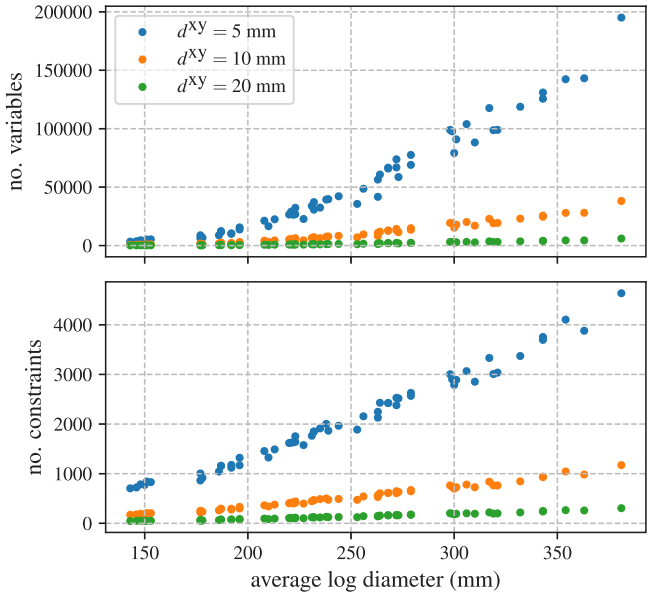

Fig. 9. Numbers of variables and constraints in the MIP models for the 2D sawing method using the evaluation function 4PointsGrade.

where the board values are directly calculated using the Grade function. Figs. 11 and 12 summarize the results in terms of value yield and CPU times (both the preprocessing time and the solution time). According to Fig. 11, using the 4PointsGrade evaluation function considerably improves the performance of the 2D sawing method: the box plot compares the value yields against SAW2010, and the bar plot compares the total value yield of all 59 logs. To demonstrate the statistical significance of this conclusion, we also carried out a paired t-test. For all three pixel sizes, we examined the null hypothesis $H_0 : \bar{V}^{4P} - \bar{V}^{W} = 0$ against alternative hypothesis $H_1 : \bar{V}^{4P} - \bar{V}^{W} > 0$, where $\bar{V}^{4P}$ and $\bar{V}^{W}$ are respectively the average value yield of the 2D sawing method with and without using the 4PointsGrade evaluation function. The test statistic corresponding to the $d^{xy} = 5$ mm, $d^{xy} = 10$ mm and $d^{xy} = 20$ mm were 11.21, 13.56, and 13.97, respectively, with a p-value almost equal to zero for all three cases. Thus, we conclude that the alternative hypothesis H_1 can be accepted with a very high confidence level.

As for the CPU times, however, Fig. 12 indicates a slight increase in the preprocessing times when using the 4PointsGrade evaluation function, while the solution time for both remains almost the same.

5.4. Sensitivity analysis of the 2D+ sawing method

To examine the effect of the segment size, d^z, on the performance of the 2D+ method, the following four scenarios are considered:

1. $d^z \in \{20, 30, 40, 50\}$ cm.
2. $d^z \in \{30, 40, 50\}$ cm.
3. $d^z \in \{40, 50\}$ cm.
4. $d^z = 50$ cm.

Under each scenario, the experiment for the corresponding d^z values can be done in parallel on separate machines. For CPU times, the maximum time is taken into account, and for value yield, the best result obtained from the corresponding d^z values is used for analysis. 2D+ sawing outperforms SAW2010 in 53 out of 59 logs under both Scenarios . Under Scenarios , this number decreases to 51 and 50 logs, respectively. The total value yield of the logs is about 15,177 SEK, 15,165 SEK, 15,125 SEK, and 15,088 SEK under Scenarios respectively, representing an improvement of 5.49% to 6.11% compared to SAW2010. We also conducted a paired t-test based on the described scenarios to examine whether there is a meaningful improvement in the average value yield of the logs when the segment size is increased. In this respect, we performed the statistical test for the following pair of scenarios: Scenarios 1 vs. Scenarios 2, Scenarios 2 vs. Scenarios 3, and Scenarios 3 vs. Scenarios 4. The corresponding test statistics for these cases were 4.14, 8.15, and 5.09, all yielding zero p-value. As a result, we can confidently conclude that there is indeed a significant improvement in the average value yield of the logs as the segment size increases.

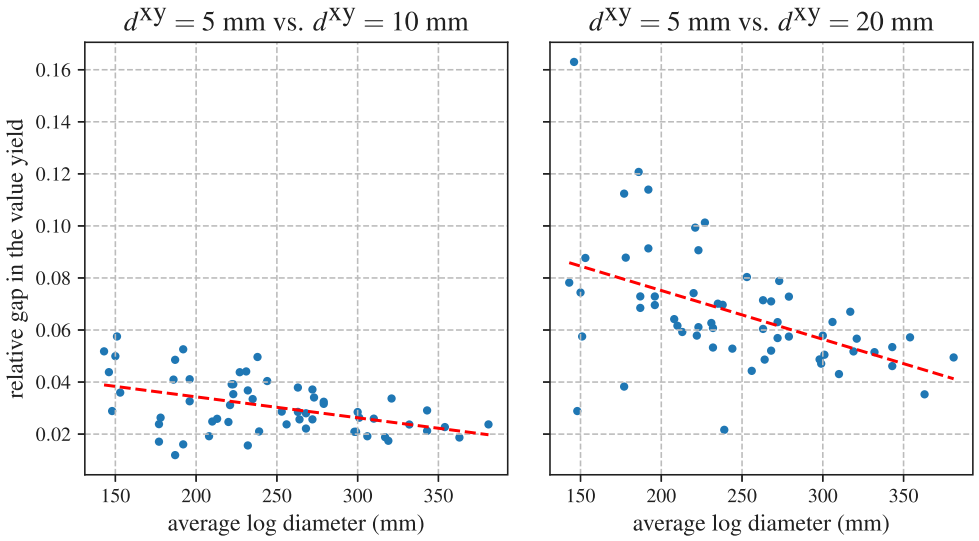

Fig. 10. Relative differences in the value yield between the 2D sawing method with 5 mm vs. 10 mm and 5 mm vs. 20 mm pixel sizes, plotted against the average log diameter (average of top and bottom diameters given in Table 3).

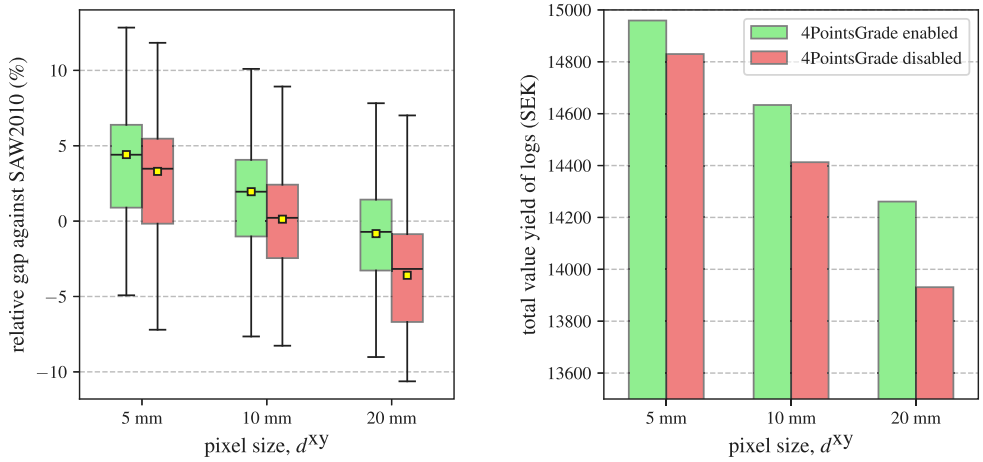

Fig. 11. Performance comparison of the 2D sawing method with and without the 4PointsGrade evaluation function.

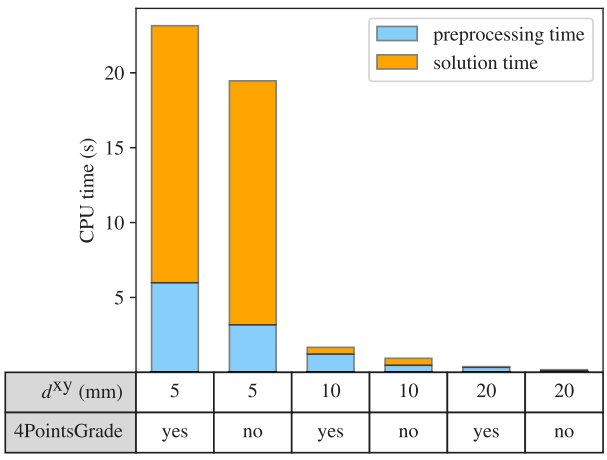

Fig. 12. Comparison of the average CPU times for the proposed 2D sawing method with different pixel sizes: 5 mm, 10 mm, and 20 mm.

The plots in Fig. 13 compare the performance of the 2D and 2D+ sawing methods in terms of average CPU time and relative gap against SAW2010. The box plot in this figure demonstrates that even with $d^z = 50$ cm (Scenario 4), the improvement achieved by the 2D+ sawing method is superior to that of the 2D sawing method. This conclusion also highlights the effectiveness of the proposed DP algorithm (which is a part of the preprocessing) in improving the value yield. However, it should be noted that applying the 2D+ sawing method comes with a considerable increase in the preprocessing time. The bar plot given in Fig. 13 shows that the solution time for both methods is almost the same, but in the 2D+ sawing method the preprocessing time increases considerably as d^z decreases. A possibility to reduce the computing time is to use a larger segment size in the 2D+ sawing method. For example, using Scenario 2 instead of Scenario 1 can decrease the average computing time by 30% with a reduction of only 0.08% in the total value yield of the logs.

5.5. Impact of saw kerf on the yield

The thickness of the saw blade is one of the influencing factors on the volume yield and the amount of sawdust produced. The development of new machinery for the implementation of flexible sawing

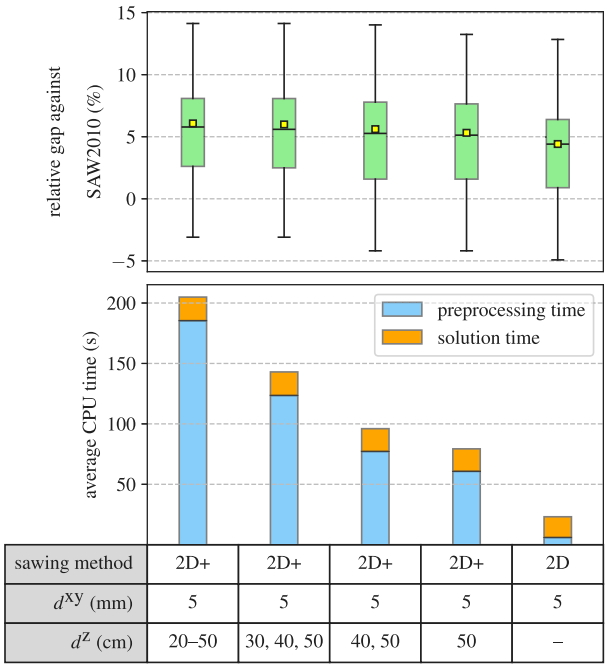

sawing method	2D+	2D+	2D+	2D+	2D
d^{xy} (mm)	5	5	5	5	5
d^{z} (cm)	20–50	30, 40, 50	40, 50	50	–

Fig. 13. Plots comparing the performance of 2D and 2D+ sawing methods under different scenarios.

schemes enables the possibility of reducing the thickness of the saw blade. It also allows more precise control over the sawing process. Assuming that in the future it will be possible to build more accurate machinery for sawing logs, the saw kerf was simply assumed to be 2 mm in the computations made in the previous sections. However, due to technological limitations, in the majority of earlier studies, the value of this parameter is assumed to be 4 mm, see for example Lundahl and Grönlund (2010), Berglund et al. (2013), Johansson (2013), Riesco Muñoz et al. (2013) and Ah Shenga et al. (2015). In this section, a comparison is made to evaluate the effect of this parameter on sawing yield. In this connection, the 2D+ sawing method is applied to the logs specified in Table 3, considering a 4 mm saw kerf.

Fig. 14 shows the volume yield per log in cubic meters (m^3) while considering a 4 mm saw kerf, shown in orange. The blue color highlights the improved volume yield when using a 2 mm saw kerf, while the gray color then represents the total wasted volume of the log, including both sawdust and unused wood. This figure demonstrates that decreasing the saw kerf from 4 mm to 2 mm results in an increase in volume yield. The overall improvement in volume yield is approximately 5% for the 59 logs. At a 4 mm saw kerf, the estimated total value yield is 14,449 SEK. However, reducing the saw kerf to 2 mm increases this value to 15,177 SEK, resulting in a gain of 1856 SEK per m^3 of raw material. These results almost align with Pinto et al. (2002)'s investigation, which found that, on average, a 1 mm decrease in saw kerf reduces the volume yield by about 3%.

6. Conclusions and future work

In this paper, we introduce two methods, namely 2D and 2D+ sawing, for solving a sawing optimization problem with the objective of maximizing the value yield through a flexible sawing scheme. Both methods address the sawing problem in two phases: the preprocessing phase, where potential sawing positions are evaluated, and the optimization phase, where a maximum set-packing problem is solved to obtain a feasible cut pattern (CP). The key difference between the 2D and 2D+ methods is the 2D+ capability for the placement of multiple boards across a log's length. To assess their effectiveness, the 2D and 2D+ methods were tested on 59 logs from the Swedish Pine Stem Bank. The 2D sawing method exhibits faster preprocessing time compared to the 2D+ sawing method, while the solution time for both methods is nearly identical. However, when considering the value yield, the 2D+ sawing method outperforms the 2D method by up to 8.9%. Additionally, the results are compared to SAW2010, an existing tool utilizing a cant sawing scheme to generate CPs. The findings indicate that employing a flexible sawing scheme can improve the value yield by up to 28.4% compared to cant sawing. On average, the 2D and 2D+ methods achieved value yield improvements of approximately 4.59% and 6.11%, respectively. While the practical implementation of a flexible sawing scheme still faces challenges in today's sawmill industry due to the limited capability of current sawmill machinery and equipment, the potential increase in value yield motivates the exploration of alternative sawmill solutions in the industry.

Based on the limitations of this paper we suggest some directions for future research. While this paper concentrates on board grading using wane as the basis, it is important to highlight that the grading rules can be expanded to include other types of defects, particularly knots. However, it should be noted that incorporating such additional defect types would increase the preprocessing time. In such scenarios, it would be worthwhile to consider exploring alternative parallel processing solutions, such as GPU processing or a hybrid CPU/GPU processing approach.

The sawing optimization problem addressed in this paper is suitable for decision making at an operational level where the objective is to optimize value yield for each log individually without taking into account board demands. However, when it comes to real-life sawmill

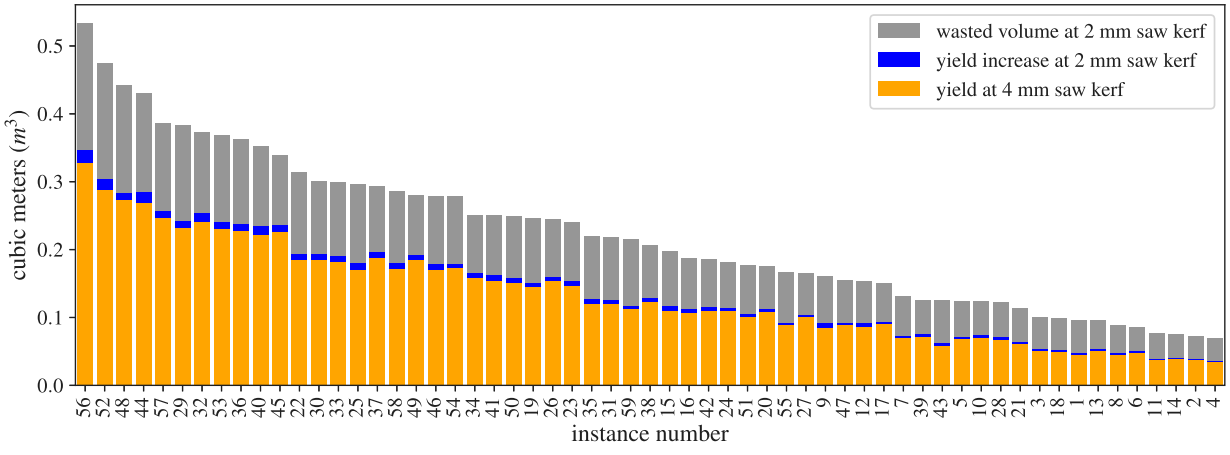

Fig. 14. Impact of 2 mm and 4 mm saw kerf on the volume yield, logs are sorted in decreasing order of volume.

Table A.1
Notation used in the development of the 2D and 2D+ sawing methods.

Sets:		*Use case*:
$\mathcal{P}$	Set of pixels in the xy-plane	2D and 2D+
$\mathcal{I}(t)$	Set of pixels where a board of type $t \in \mathcal{T}$ can be sawed	2D
$\mathcal{S}(p)$	Set of pairs $(t, p') \in \mathcal{T} \times \mathcal{P}$ that overlap with pixel $p \in \mathcal{P}$	2D
$\mathcal{B}$	Set of block sizes	2D+
$\mathcal{T}^+(b)$	Set of board types that fit only into a block of size $b \in \mathcal{B}$	2D+
$\mathcal{K}$	Set of log segments	DP
$\mathcal{C}$	Set of pairs $(k, k') \in \mathcal{K}^2$ that meet the requirement on minimum board length	DP
$\mathcal{I}^+(p)$	Set of pixels where a block of size $b \in \mathcal{B}$ can be sawed	2D+
$\mathcal{S}^+(p)$	Set of pairs $(p', b) \in \mathcal{P} \times \mathcal{B}$ containing pixel $p \in \mathcal{P}$	2D+
Indices:		
p, p'	Index of pixels	2D and 2D+
b, b'	Index of blocks	2D+
k, k'	Index of log segments	DP
c	Index of segment pairs	DP
s	Index of steps	DP
Parameters:		
d^{xy}	Pixel size in the xy-plane	2D and 2D+
d^{z}	Segment size across the z-axis	2D+
M	Number of steps	DP
z_k^0	Starting slice of log segment $k \in \mathcal{K}$	DP
z_k^1	Ending slice of log segment $k \in \mathcal{K}$	DP
v_{tp}	Value of board type $t \in \mathcal{T}$ at pixel $p \in \mathcal{P}$	2D
v_{pb}^+	Value of block size $b \in \mathcal{B}$ at pixel $p \in \mathcal{P}$	2D+
Decision variables:		
x_{tp}	= 1 if a product of type $t \in \mathcal{T}$ is sawed at pixel $p \in \mathcal{P}$, otherwise 0	2D sawing model
x_{pb}^+	= 1 if a block of size $b \in \mathcal{B}$ is sawed at pixel $p \in \mathcal{P}$, otherwise 0	2D+ sawing model

planning it is also important to take into account customer demand. In such circumstances, it would be interesting to integrate the proposed problem with production planning and scheduling problems.

Finally, to enhance the value yield, the sawing optimization problem can be expanded by introducing greater flexibility in board sawing variables, including skew and rotation. However, this expansion would result in a substantial rise in the number of potential sawing positions, making the proposed methods less effective. To tackle this issue, alternative optimization techniques, such as heuristics and metaheuristic algorithms, may be considered in future studies.

CRediT authorship contribution statement

Kamran Forghani: Writing – original draft, Visualization, Validation, Software, Methodology, Investigation, Formal analysis. **Mats Carlsson:** Writing – review & editing, Methodology, Investigation, Funding acquisition, Conceptualization. **Pierre Flener:** Writing – review & editing, Validation, Methodology, Investigation, Conceptualization. **Magnus Fredriksson:** Writing – review & editing, Resources, Project administration, Methodology, Investigation, Funding acquisition, Data curation, Conceptualization. **Justin Pearson:** Writing – review & editing, Methodology, Investigation, Conceptualization. **Di Yuan:** Writing – review & editing, Supervision, Project administration, Methodology, Funding acquisition, Conceptualization.

Declaration of competing interest

The authors declare that they have no known competing financial interests or personal relationships that could have appeared to influence the work reported in this paper.

Data availability

Data will be made available on request.

Acknowledgment

This work was supported by Sweden's Innovation Agency (VINNOVA) via BioInnovation under grant 2020–03734.

Appendix A. Additional notation

See Table A.1.

Appendix B. Initialization procedure

Procedure Initialize(Method)

1 $\mathcal{P} \leftarrow \left\{(i,j) \in \mathbb{N}_0^2 \mid i < \frac{W}{d^{\text{xy}}},\ j < \frac{H}{d^{\text{xy}}}\right\}$
2 **switch** Method **do**
3 **case** 2D Sawing **do**
4 $\mathcal{I}(t) \leftarrow \{\},\ \forall t \in \mathcal{T}$ // these sets will grow in Line 11 of Algorithm 1
5 $\mathcal{S}(p) \leftarrow \{\},\ \forall p \in \mathcal{P}$ // these sets will grow in Line 15 of Algorithm 1
6 **case** 2D+ Sawing **do**
7 $\mathcal{B} \leftarrow \left\{(m,n) \in \mathbb{N}^2 \mid m \le \left\lceil \max_{t\in\mathcal{T}} \left\{\frac{w_t+g}{d^{\text{xy}}}\right\}\right\rceil,\ n \le \left\lceil \max_{t\in\mathcal{T}} \left\{\frac{h_t+g}{d^{\text{xy}}}\right\}\right\rceil\right\}$
8 $\mathcal{T}^+(b) \leftarrow \left\{t \in \mathcal{T} \mid \left\lceil\frac{w_t+g}{d^{\text{xy}}}\right\rceil = m,\ \left\lceil\frac{h_t+g}{d^{\text{xy}}}\right\rceil = n,\ (m,n) = b\right\},\ \forall b \in \mathcal{B}$
9 $\mathcal{K} \leftarrow \left\{1, 2, \ldots, \left\lceil\frac{N}{d^{\text{z}}}\right\rceil\right\}$
10 $z_k^0 \leftarrow (k-1)d^{\text{z}} + 1,\ \forall k \in \mathcal{K}$
11 $z_k^1 \leftarrow \min\{N, k \cdot d^{\text{z}}\},\ \forall k \in \mathcal{K}$
12 $\mathcal{C} \leftarrow \left\{(k,k') \in \mathcal{K}^2 \mid k' \ge k,\ (z_{k'}^1 - z_k^0 + 1)L^{\text{z}} \ge L^{\min}\right\}$
13 $M \leftarrow \min\left\{|\mathcal{K}|, \left\lfloor\frac{N \cdot L^{\text{z}}}{L^{\min}}\right\rfloor\right\}$
14 $\mathcal{I}^+(p) \leftarrow \{\},\ \forall p \in \mathcal{P}$ // these sets will grow in Line 6 of Algorithm 2
15 $\mathcal{S}^+(p) \leftarrow \{\},\ \forall p \in \mathcal{P}$ // these sets will grow in Line 10 of Algorithm 2

References

Ah Shenga, P.A., Bomark, P., Broman, O., Sandberg, D., 2015. Simulation of tropical hardwood processing: Sawing methods, log positioning, and outer shape.

BioResources 10 (4), 7640–7652. http://dx.doi.org/10.15376/biores.10.4.7640-7652.
Ah Shenga, P., Bomark, P., Broman, O., Sandberg, D., 2016. The effect of log position accuracy on the volume yield in sawmilling of tropical hardwood. BioResources 11 (4), 9560–9571. http://dx.doi.org/10.15376/biores.11.4.9560-9571.
Berglund, A., Broman, O., Grönlund, A., Fredriksson, M., 2013. Improved log rotation using information from a computed tomography scanner. Comput. Electron. Agric. 90, 152–158. http://dx.doi.org/10.1016/j.compag.2012.09.012.
Bhandarkar, S.M., Faust, T.D., Tang, M., 2002. Design and prototype development of a computer vision-based lumber production planning system. Image Vis. Comput. 20 (3), 167–189. http://dx.doi.org/10.1016/S0262-8856(01)00087-7.
Bommathanahalli, A., Xie, M., Yun, Z., Sun, J.C., Lei, Z., Allen, G., 2007. TOPSAW sawing optimization analysis using grid computing. In: Second Int. Multi-Symp. Comput. Comput. Sci.. IEEE, pp. 228–234. http://dx.doi.org/10.1109/IMSCCS.2007.80.
Bouzid, M.C., Salhi, S., 2020. Packing rectangles into a fixed size circular container: Constructive and metaheuristic search approaches. European J. Oper. Res. 285 (3), 865–883. http://dx.doi.org/10.1016/j.ejor.2020.02.048.
Breinig, L., Broman, O., Brüchert, F., Becker, G., 2015. Optimization potential for perception-oriented appearance classification by simulated sawing of computed tomography-scanned logs of Norway spruce. Wood Mater. Sci. Eng. 10 (4), 319–334. http://dx.doi.org/10.1080/17480272.2014.977944.
Correa, C.A., Maldonado, M.R., Lozano, D.M., Carrasco, C.A., 2014. 3D optimization of cutting patterns for logs of Pinus radiata d. don with cylindrical defective core. In: 10th Int. Conf. Model. Optim. Simul.. Nancy, France, p. 8, URL: https://hal.science/hal-01166645.
Dolan, E.D., Moré, J.J., 2002. Benchmarking optimization software with performance profiles. Math. Program. 91, 201–213. http://dx.doi.org/10.1007/s101070100263.
Fredriksson, M., 2012. Reconstruction of pinus sylvestris knots using measurable log features in the Swedish pine stem bank. Scand. J. For. Res. 27 (5), 481–491. http://dx.doi.org/10.1080/02827581.2012.656142.
Fredriksson, M., 2014. Log sawing position optimization using computed tomography scanning. Wood Mater. Sci. Eng. 9 (2), 110–119. http://dx.doi.org/10.1080/17480272.2014.904430.
Fredriksson, M., 2015. Optimizing sawing of boards for furniture production using CT log scanning. J. Wood Sci. 61 (5), 474–480. http://dx.doi.org/10.1007/s10086-015-1500-0.
Fredriksson, M., Bomark, P., Broman, O., Grönlund, A., 2015. A trapeze edging method for cross laminated timber panel production. In: Proc. 22nd Int. Wood Machin. Semin.. Universite Laval, pp. 323–332.
Gergel', T., Sedliak, M., Bucha, T., Oravec, M., Slamka, M., Pástor, M., 2020. Prediction model of wooden logs cutting patterns and its efficiency in practice. Appl. Sci. 10 (9), 3003. http://dx.doi.org/10.3390/app10093003.
Grönlund, A., Björklund, L., Grundberg, S., Berggren, G., 1995. Manual för Furustambank [Manual for Pine Stem Bank]. Luleå tekniska universitet, (In Swedish).
Hinostroza, I., Pradenas, L., Parada, V., 2013. Board cutting from logs: Optimal and heuristic approaches for the problem of packing rectangles in a circle. Int. J. Prod. Econ. 145 (2), 541–546. http://dx.doi.org/10.1016/j.ijpe.2013.04.047.
Hosseini, S.M., Peer, A., 2022. Wood products manufacturing optimization: A survey. IEEE Access 10, 121653–121683. http://dx.doi.org/10.1109/ACCESS.2022.3223053.
Johansson, E., 2013. Computed Tomography of Sawlogs: Knot Detection and Sawing Optimization (Ph.D. thesis). Luleå University of Technology, Wood Science and Engineering, p. 116.
Khaloian Sarnaghi, A., Rais, A., Kovryga, A., Gard, W., van de Kuilen, J., 2020. Yield optimization and surface image-based strength prediction of beech. Eur. J. Wood Wood Prod. 78, 995–1006. http://dx.doi.org/10.1007/s00107-020-01571-4.
Lin, W., Wang, J., 2012. An integrated 3D log processing optimization system for hardwood sawmills in central appalachia, USA. Comput. Electron. Agric. 82, 61–74. http://dx.doi.org/10.1016/j.compag.2011.12.014.
Lin, W., Wang, J., Thomas, E., 2011. Development of a 3D log sawing optimization system for small sawmills in central Appalachia, US. Wood Fiber Sci. 43 (4), 379–393.
Lindner, B.G., Vlok, P., Wessels, C.B., 2015. Determining optimal primary sawing and ripping machine settings in the wood manufacturing chain. South. For. J. For. Sci. 77 (3), 191–201. http://dx.doi.org/10.2989/20702620.2014.1001678.
López, C.O., Beasley, J.E., 2018. Packing unequal rectangles and squares in a fixed size circular container using formulation space search. Comput. Oper. Res. 94, 106–117. http://dx.doi.org/10.1016/j.cor.2018.02.012.
Lundahl, C.G., Grönlund, A., 2010. Increased yield in sawmills by applying alternate rotation and lateral positioning. For. Prod. J. 60 (4), 331–338. http://dx.doi.org/10.13073/0015-7473-60.4.331.
Morneau-Pereira, M., Arabi, M., Gaudreault, J., Nourelfath, M., Ouhimmou, M., 2014. An optimization and simulation framework for integrated tactical planning of wood harvesting operations, wood allocation and lumber production. In: 10th Int. Conf. Model. Optim. Simul.. Nancy, France, p. 12, URL: https://hal.science/hal-01166620.
Nordmark, U., 2005. Value Recovery and Production Control in the Forestry-Wood Chain Using Simulation Technique (Ph.D. thesis). Luleå University of Technology, Luleå, Sweden.
Nordmark, U., Oja, J., 2004. Prediction of board values in Pinus sylvestris sawlogs using X-ray scanning and optical three-dimensional scanning of stems. Scand. J. For. Res. 19 (5), 473–480. http://dx.doi.org/10.1080/02827580410030172.
Parra Galvez, J.L.A., Borenstein, D., da Silveira Farias, E., 2018. Application of optimization for solving a sawing stock problem with a cant sawing pattern. Optim. Lett. 12, 1755–1772. http://dx.doi.org/10.1007/s11590-017-1178-x.
Pereira, I.P.-S.K.-H., Usenius, A., 2006. Simulated and realised industrial yields in sawing of maritime pine (Pinus pinaster ait). Eur. J. Wood Wood Prod. 64, 30–36. http://dx.doi.org/10.1007/s00107-005-0042-3.
Pinto, I., Pereira, H., Usenius, A., 2002. Sawing simulation of pinus pinaster ait. In: Proc. 4th Workshop Connect. Silvicult. Wood Qual. Model. Approach. Simul. Softw.. Association for Computing Machinery, British Columbia, Canada, INRA, Nancy, URL: http://lib.tkk.fi/Diss/2004/isbn9513863743/article3.pdf.
Pradenas, L., Garcés, J., Parada, V., Ferland, J., 2013. Genotype–phenotype heuristic approaches for a cutting stock problem with circular patterns. Eng. Appl. Artif. Intell. 26 (10), 2349–2355. http://dx.doi.org/10.1016/j.engappai.2013.08.003.
Rais, A., Ursella, E., Vicario, E., Giudiceandrea, F., 2017. The use of the first industrial X-ray CT scanner increases the lumber recovery value: Case study on visually strength-graded douglas-fir timber. Ann. for. Sci. 74 (2), 1–9. http://dx.doi.org/10.1007/s13595-017-0630-5.
Riesco Muñoz, G., Remacha Gete, A., Gasalla Regueiro, M., 2013. Variation in log quality and prediction of sawing yield in oak wood (Quercus robur). Ann. for. Sci. 70, 695–706. http://dx.doi.org/10.1007/s13595-013-0314-8.
Shenga, P.A., Bomark, P., Broman, O., Sandberg, D., 2017. Log sawing positioning optimization and log bucking of tropical hardwood species to increase the volume yield. Wood Mater. Sci. Eng. 12 (4), 257–262. http://dx.doi.org/10.1080/17480272.2016.1275788.
Shevchenko, S., Suska, A., Gradiskiy, Y., Zaslavska, N., Babich, A., 2019. Computer optimization of schematic model for sawing a log into rectangular and trapezoidal cross-section boards for panel products. Int. J. Adv. Trends Comput. Sci. Eng. 8 (6), 2944–2950. http://dx.doi.org/10.30534/ijatcse/2019/43862019.
Silva, A., Coelho, L.C., Darvish, M., Renaud, J., 2021. A Branch-and-Cut and a Parallel Algorithm for Packing Two-Dimensional Rectangles in a Circular Container. Faculté des sciences de l'administration, Université Laval, http://dx.doi.org/10.13140/RG.2.2.24035.27689.
Silva, A., Coelho, L.C., Darvish, M., Renaud, J., 2022. A cutting plane method and a parallel algorithm for packing rectangles in a circular container. European J. Oper. Res. 303 (1), 114–128. http://dx.doi.org/10.1016/j.ejor.2022.02.023.
Stängle, S.M., Brüchert, F., Heikkila, A., Usenius, T., Usenius, A., Sauter, U.H., 2015. Potentially increased sawmill yield from hardwoods using X-ray computed tomography for knot detection. Ann. for. Sci. 72, 57–65. http://dx.doi.org/10.1007/s13595-014-0385-1.
Swedish Wood, 2020. Commercial Grading of Timber, first ed. Swedish Wood, URL: https://www.swedishwood.com/publications/list%5Fof%5Fswedish%5Fwoods%5Fpublications/commercial-grading-of-timber.
Thomas, R.E., 2012. RAYSAW: A log sawing simulator for 3D laser-scanned hardwood logs. In: Proc. 18th Cent. Hardw. for. Conf.. pp. 26–28.
Todoroki, C., Rönnqvist, M., 2002. Dynamic control of timber production at a sawmill with log sawing optimization. Scand. J. For. Res. 17 (1), 79–89. http://dx.doi.org/10.1080/028275802317221118.
Tole, K., Moqa, R., Zheng, J., He, K., 2023. A simulated annealing approach for the circle bin packing problem with rectangular items. Comput. Ind. Eng. 176, 109004. http://dx.doi.org/10.1016/j.cie.2023.109004.
Ursella, E., Giudiceandrea, F., Boschetti, M., 2018. A fast and continuous CT scanner for the optimization of logs in a sawmill. In: 8th Conf. Ind. Comput. Tomogr., Vol. 23. e-Journal of Nondestructive Testing, Wels, Austria, p. 5, URL: https://www.ndt.net/search/docs.php3?id=21911.
Vanzetti, N., Broz, D., Corsano, G., Montagna, J.M., 2018. An optimization approach for multiperiod production planning in a sawmill. For. Policy Econ. 97, 1–8. http://dx.doi.org/10.1016/j.forpol.2018.09.001.
Vanzetti, N., Broz, D., Corsano, G., Montagna, J.M., 2019. A detailed mathematical programming model for the optimal daily planning of sawmills. Can. J. For. Res. 49 (11), 1400–1411. http://dx.doi.org/10.1139/cjfr-2019-0144.
Vergara, F.P., Palma, C.D., Sepúlveda, H., 2015. A comparison of optimization models for lumber production planning. Bosque (Valdivia) 36, 239–246. http://dx.doi.org/10.4067/S0717-92002015000200009.
Wery, J., Gaudreault, J., Thomas, A., Marier, P., 2018. Simulation-optimisation based framework for sales and operations planning taking into account new products opportunities in a co-production context. Comput. Ind. 94, 41–51. http://dx.doi.org/10.1016/j.compind.2017.10.002.
Wessels, C.B., 2009. Cant sawing log positioning optimization: A simulation study. For. Prod. J. 59 (4).
Yun, Z., Chang, S.J., Lei, Z., Allen, G., Bommathanahalli, A., 2008. Grid-enabled sawing optimization: From scanning images to cutting solution. In: Proc. 15th ACM Mardi Gras Conf.. Association for Computing Machinery, New York, USA, pp. 1–8. http://dx.doi.org/10.1145/1341811.1341829.